Cano-Pleite, E., Hernández-Jiménez, F. & Acosta-Iborra, A. (2017). Bulk oscillation and velocity wave propagation in a vibrated fluidized bed at minimum fluidization conditions. *Powder Technology*, vol. 308, pp. 346–361.

DOI: 10.1016/j.powtec.2016.12.031

Bulk oscillation and velocity wave propagation in a vibrated fluidized bed at minimum fluidization conditions

E. Cano-Pleite[a,*], F. Hernández-Jiménez[a], A. Acosta-Iborra[a]

[a] *Department of Thermal and Fluid Engineering, Carlos III University of Madrid, Av. de la Universidad 30, 28911, Leganés, Madrid, Spain*

Abstract

The present work experimentally characterizes the behavior of the bed bulk and the solids velocity in a vertically vibrated pseudo-2D fluidized bed operated at minimum fluidization conditions. Measurements are undertaken combining Digital Image Analysis (DIA) and Particle Image Velocimetry (PIV). Vibration at different amplitudes and frequencies is applied to the bed by the use of two vibro-motors symmetrically disposed at both sides of the bed vessel. The results show that both the center of mass of the bed and the bed surface oscillate with a frequency equal to that of the bed vessel. The bed surface oscillates in opposition of phase with the bed vessel, which reflects a cyclic compression and expansion of the bed bulk. The average solids velocity at each oscillation phase clearly shows that there exist a compression wave, produced by the impact of the bed bulk with the gas distributor, and an expansion wave, produced by the expansion of the bed bulk. Both waves travel upwards the bed bulk perturbing the velocity of particles along the bed height. The waves span all the bed width and separate the bed bulk into two clearly distinguishable regions with different relative velocities. When the particles belonging to the region under the wave move upwards, the particles in the region above the wave move downwards and vice versa. The results also reveal that the compression wave generated at the bottom of the bed propagates at a velocity similar to the reported velocity of sound inside a fluidized bed. Far from the distributor, this wave velocity resulted to be nearly independent of the vibration amplitude and frequency for the range of conditions tested. These results can be useful for the understanding of the behavior of particles and bubbles in vibrated fluidized beds.

Keywords: Fluidized bed, Vibration, Bulk, Pseudo-2D, PIV, Wave

1. Introduction

Many key operations in the chemical, energy and process industries rely on gas-solid fluidized beds because of their high contact area, homogeneity, heat and mass transfer rates and solids handling capabilities [1]. Among these operations are fluid catalytic cracking (FCC), gasification, combustion of solid fuels,

*Corresponding author. Tel:+34 91 624 8884
Email address: edcanop@ing.uc3m.es (E. Cano-Pleite)

Fischer-Tropsch synthesis, drying, granulation and coating [2]. However, fluidized beds have not yet reached their full potential owing to gas channeling, agglomeration, defluidization and segregation of particles, among other problems arising in real operation. To diminish or eliminate these problems, the gas fluidized bed can be forced to vibrate creating a 'vibrated fluidized bed' (VFB). Vibration is commonly applied by mechanically shaking the bed vessel, which transmits its vibration to the particles of bed [3–6].

Vibration of a gas fluidized bed tends to break gas channeling and agglomeration, facilitate fluidization and enhance mixing or segregation depending on the vibration strength. Vibration is also a way of stabilizing the system and gain some control on the bed dynamics [7–11]. Despite its advantages, vibration introduces complexities in the dynamics of the bed that are far from being fully understood. Knowledge of these complex physical phenomena arising from vibration of a fluidized bed could be used to improve design and control of the existing VFBs and to increase its range of operation to new applications.

There is an ongoing effort to understand the behavior of VFB both experimentally and numerically. Some works have studied the effect that vibration possesses on the general dynamics of the fluidized bed. Mawatari et al. [7] observed experimentally that the minimum fluidization velocity decreased when adding vibration to a conventional fluidized bed. Zhou et al. [11] studied the effect of different vibration modules (vertical, horizontal and twist) on the bed dynamics. The size and distribution of bubbles in a vibrated fluidized bed has been also extensively analyzed in previous works [12–16]. Eccles and Mujumdar [12] studied the effect of vibration on a train of bubbles. In Zhou et al. [14, 15] the behavior of bubbles passing through two fringes of 2 cm in the upper half of the bed is investigated. They observed that the bubble diameter and velocity increase when the system is vibrated. Mawatari et al. [13] also studied the bubble diameter and velocity in a VFB. They showed that for sufficiently large vibration strengths, vibration promoted a change in the flow pattern and that affected the bubble behavior. A change of the flow pattern with vibration was also observed by Cano-Pleite et al. [16], in which they also studied the bubble behavior for a wide range of operating conditions and for three different particle diameters. The results in [16] show that the bubble behavior is different in the upper and lower sections of the bed, which suggests the presence of waves changing the way the bubbles behave along the bed.

In general, experimental studies analyzing the bed and bubble behavior in VFBs make use of pseudo two-dimensional beds (i.e. beds of small thickness), which have shown to be of great importance for the understanding of fluidized beds [17, 18]. Among the different experimental techniques aimed at understanding the bed and bubble behavior, Digital Image Analysis (DIA) is one of the most used in VFBs [11–15, 19]. However, although it has demonstrated to be of great use in conventional fluidized beds [17, 18, 20], the use of Particle Image Velocimetry (PIV) in VFBs is still very reduced [21]. Zeilstra et al. [21] studied, by means of PIV and discrete particle simulations, the solids velocity in a vibrated fluidized bed operated in bubbling regime. However, only averaged values concerning mean and RMS velocities of solids in the bed are discussed, which precludes the extraction of time-resolved conclusions on the particle behavior in the

bed.

Numerical models have been also widely employed for a better understanding of the bed dynamics in VFBs. Generally, discrete models are used for the simulation this kind of beds [22–24]. Tatemoto et al. [22] and Xiang et al. [23] employed a Lagrangian-Eulerian (CFD-DEM) method for the simulation of the particle motion in vibrated fluidized beds operated in two-dimensional beds. In [22], the effect of vibration on the change of void fraction and pressure fluctuations as a function of time was carried out. Xiang et al. [23] studied the distribution of concentration and velocity of particles in the bed. They observed that the vibration energy is transmitted by collisions between the particles and the distributor when the bed is accelerating, whereas there exists a wave propagation through the bed when the bed is decelerating. Limtrakul et al. [24] studied the effect of vibration on the motion and velocity of 3D simulations of a cylindrical bed filled with cohesive particles. More recently Acosta-Iborra et al. [25] developed a new methodology for the simulation of VFBs by means of an Euler-Euler method (two fluid model). This method was used in [26] for the simulation of the motion of an isolated bubbles in a VFB under the same conditions of [19]. They observed that the use of a compressible gas model leaded to the presence of a phase delay of bubble characteristics between the upper and the lower halves of the bed, whereas the incompressible model yielded to unrealistic results. Although there has been a significant progress in the numerical simulation of VFBs, there still exists a need of further experimental data to validate models and improve the existing ones.

The presence of pressure waves in conventional fluidized beds has also been a field of great interest during the last decades [27–31]. However, works analyzing the wave propagation mechanisms in a VFB remain scarce [32–34]. Wang et al. [32] studied the wave propagation in both a packed and a fluidized bed operated in bubbling regime. In their results, when the gas superficial velocity was below the minimum fluidization velocity, the interaction between the bed bulk and the distributor was by collision occurring locally at the base of the bed. However, when $U > U_{mf}$, the action of vibration on the bed was found to be through a continuous wave propagation in a pseudo-continuous and pseudo-elastic medium. The wave propagation mechanism was further studied by Wang et al. [33] in a bed operated in bubble regime. By means of a set of pressure probes situated at different heights from the distributor they calculated the wave velocity to be in the range 9-75 m/s. Barletta et al. [34] experimentally studied the dynamic response of a vibrated fluidized bed filled with two different types of particles. The results showed an opposition of phase between the bed vessel oscillation and the free surface of the bed for a wide range of operating conditions, which suggests a cyclic compression and expansion of the bed bulk. The results shown in [34] are in agreement with recent studies on the oscillatory motion of the bed bulk and, also, of isolated bubbles in a vertically vibrated fluidized bed [19, 26]. In Cano-Pleite et al. [19] the bubble diameter and velocity oscillated with a frequency equal to that of the bed vessel. Besides, the presence of a phase delay of bubble characteristics between the upper and the lower sections of the bed suggested the presence of compression-expansion waves

changing the wave the bubbles behave along the bed height.

Therefore, in view of the previously cited references, one crucial aspect to characterize is the oscillating movement of the particles in a VFB, as they seem to influence both the bed bulk and the bubbles dynamics. In particular, oscillations of the particle movement in a VFB may be linked to the compression and expansion of the bulk of the bed, which in turn can affect the size and rise velocity of bubbles and the resulting gulf stream motion. Besides, it is not totally clear the way vibration is propagated by the particle movement in the bulk of a gas fluidized bed. All these effects can have an impact on processes like gasification, combustion, drying and granulation in VFBs. From a fundamental point of view, it is also interesting to know the temporal and spatial distribution of the particle movement in the bed and how this movement is coupled with the oscillation of the bed bulk. These results can be also of interest for the validation and development of numerical models describing the dynamics of VFBs.

The aim of the present work is twofold. Firstly, the oscillations of the free surface, center of mass and bulk of a vibrated pseudo-2D bed, fluidized with gas at minimum fluidization, will be experimentally characterized with DIA. Operation at minimum fluidization will eliminate the disturbance of bubbles on the dense phase, facilitating the measurement of the impact of vibration on the bulk of a fluidized the bed. Secondly, these observations will be connected with the temporal and spatial distribution of the particle movement obtained with PIV measurements in the studied VFB. The ultimate objective of all these results is to explain the link between the bed bulk oscillation and the particle movement, and to present detailed information of the oscillating velocity of particles that may help researchers to understand VFB and improving existing models of its behavior.

2. Experimental setup

The experimental facility used in the present work consisted on a pseudo-2D bed of dimensions 0.3 x 0.6 x 0.01 m (width W, height H and thickness K, respectively), which was placed on a vibrating structure. Figure 1 shows a sketch of the experimental facility employed. The front and rear walls of the bed were made of glass and the rear wall was painted in black to increase contrast of the front images. The fluidizing gas was air, which was injected to the bed through a gas distributor consisting on 20 aligned holes of 1 mm that are spaced 1.5 cm apart. The bed material was ballotini glass beads with a density of 2500 kg/m^3 and a diameter range between 425-600 μm. This bed material corresponds to type B particles, according to Geldart's classification [35]. Approximately, 5% of the particles were painted black to enhance the correlation during the processing of results with Particle Image Velocimetry (PIV). The gas mass flow was measured by means of a mass flow meter with a resolution of 2 L/min (0.01 m/s). The minimum fluidization velocity of the particles at static conditions was $U_{mf} = 0.28$ m/s, which was measured by using the mean value of the pressure signal of a pressure probe attached to the rear wall at 0.025 m above the distributor.

[Figure 1 about here.]

Vibration was induced into the bed by means of two vibro-motors (Italvibras MVSI 10/310 SO2) symmetrically placed at each side of the bed, which produced a sinusoidal displacement of the bed vessel, $\delta(t) = A\sin(2\pi f)$. The amplitude of vibration, A, was varied by changing the relative position of the two pair of eccentric masses inside each of the vibro-motors. The frequency of vibration, f, was controlled by changing the turning velocity of the motors. More details about the experimental facility can be found in [19].

A high speed camera (Redlake Motion pro X3) was employed to record images of the front view of the bed bulk at a frame rate of 250 images per second. The camera was mounted on a tripod that was not subjected to vibration. Two spotlights were symmetrically placed a each side of the bed to provide a uniform illumination of the bed bulk. In order to calculate the bed displacement at every time instant, and similarly to [19], five small white squares serving as a reference were glued under the base of the bed. The vertical instantaneous position of the bed was obtained from the centroid location of each of the reference squares, which was calculated by means of DIA. The frequency of vibration of the bed vessel was obtained by performing a frequency domain analysis (Welch periodogram) of the instantaneous position of the bed. Since the bed vessel followed a sinusoidal displacement, the equivalent amplitude and velocity of vibration of the bed vessel for each experiment was calculated as:

$$A = \sigma_{\delta(t)}\sqrt{2} \tag{1}$$

$$V = \sigma_{v(t)}\sqrt{2} \tag{2}$$

where $\delta(t)$ is the instantaneous bed vessel displacement, $v(t) = d\delta(t)/dt$ is the instantaneous velocity of the bed vessel and σ is the standard deviation of the time evolution of δ or v with regard to their mean.

Each of the conducted experiments comprised a recording time of approximately 15 seconds. Firstly, the gas superficial velocity was adjusted for each experiment to set minimum fluidization conditions. Secondly, the vibration of the bed was activated. Images started to be recorded approximately 10 seconds after turning on the vibro-motors in order to avoid the recording of start-up effects.

Table 1 lists the experimental conditions of the experiments carried out. Three different static bed heights (H_0) were tested: 0.3 m, 0.375 m and 0.45 m, which correspond to H_0/W=1, 1.25 and 1.5, respectively. The selected base case was Exp. 1, which has the largest frequency allowed by the vibro-motors (f =17.1 Hz), the largest static bed height (H_0/W=1.5) and an intermediate amplitude A = 4.1 mm. These conditions were found to clearly show the main features of the bed bulk behavior. The effects of the vibration amplitude and frequency were analyzed by independently varying f or A for the largest static bed height $H_0/W = 1.5$. Table 1 also includes the value of the vibration strength parameter for each of the experiments, which is

defined as the ratio of the vibration acceleration to the acceleration of gravity:

$$\Lambda = \frac{A(2\pi f)^2}{g} \tag{3}$$

[Table 1 about here.]

3. Data processing

3.1. Digital Image Analysis

A constant threshold [36] was used to transform the grayscale images captured by the high speed camera into black and white images. This threshold assigns, for each pixel in the image, a value of either 1 (white, dense phase) or 0 (black, out of the bed). Once the image was thresholded, the center of mass, the area of the bed (i.e. the area occupied by white pixels) and the position of the bed surface could be calculated by means of Digital Image Analysis (DIA) techniques. PIV calculations were carried out with the pixels of the bed image that were previously recognized as dense phase.

3.2. Average oscillation of the bed bulk

An averaging of cycles method is employed for the study of the oscillatory behavior of the bulk velocity, the bed surface and the bed center of mass [19, 26]. This oscillation is obtained with DIA in the experiments and can be expressed in a relative (to the distributor) or absolute system of reference. The instantaneous oscillation of a given variable z can be calculated as

$$\Delta z(t) = z(t) - \widehat{z}(t) \tag{4}$$

where $z(t)$ is the time series of the variable under study and $\widehat{z}(t)$ is the local average of z over a time interval $[-T/2, T/2]$, with $T = 1/f$ being the time period of oscillation.

Each instantaneous value of $\Delta z(t)$ is associated to a phase ϕ, where $\phi = 0$ corresponds to the beginning of a cycle (bed vessel at its central position, $\delta(t_0) = 0$, and moving upwards) and $\phi = 2\pi$ to the end of the cycle (bed vessel at its central position, $\delta(t_0 + T) = 0$, and moving again upwards). Thus, for every image in the experiment, a data point in the phase domain ($\phi = 0 - 2\pi$) is obtained. It was observed that both the bed center of mass and the bed surface presented a cyclic motion resembling a sinusoidal displacement (see Figure 2). To enhance the visual inspection of the results, a polynomial fitting of order 20 is proposed for the oscillation of the center of mass and the surface of the bed. However, the local bed bulk velocity, especially close to the distributor, presented a cyclic displacement whose behavior differed from that of a sinusoidal displacement. Thus, a smoothing spline of Δz was chosen to represent the results of the velocity oscillation in the interval $\phi = 0 - 2\pi$.

3.3. Particle Image Velocimetry

The velocity of the bed particles at an instant between each two consecutively recorded images was obtained by means of PIV, which is based on the cross−correlation of consecutive images. For that, the multigrid code MATPIV [37] was used. A final interrogation window of 32x32 pixels and 50% overlapping was employed for the calculation of the velocity of particles in the bed.

The bed bulk velocities were analyzed as a function of the vibration phase. It was observed that the oscillation of the bed bulk presented a cyclic behavior with a period equal to the period of oscillation of the bed vessel, $T = 1/f$. As the bed manifests a cyclic behavior, the time dependence of the velocity vectors of the bed bulk can be reduced to a function of the phase $\phi = 2\pi(t - t_0)f$ comprising a given oscillation $[t_0, t_0 + T]$, as done in Section 3.2. Thus, the complete period of oscillation of the bed bulk, T, was divided into M phase intervals of phase $\phi \in [0, 2\pi]$ to capture the oscillatory behavior of the bed bulk as a function of the bed vessel phase. The velocity vectors pertaining to a given phase interval were averaged, obtaining a velocity map for each of the phase intervals in which the period of oscillation is divided. Hence, the average velocity of the bed bulk in every phase interval can be calculated as:

$$U_{s,\phi_k}(x, y) = \frac{\sum_{i=1}^{N} U_{s,i}(x, y)\delta_{i,k}}{\sum_{i=1}^{N} \delta_{i,k}} \tag{5}$$

where N is the number of frames along an experiment and $\delta_{i,k}$ is equal to the unity if the phase ϕ_i in the i^{th} frame is within the k^{th} interval of phase:

$$\delta_{i,k} = \begin{cases} 1 & \text{if } \frac{2(k-1)}{M}\pi < \phi_i < \frac{2k}{M}\pi \\ 0 & \text{otherwise} \end{cases} \tag{6}$$

As commented in the previous section, the solids velocity can be referred to a relative system of reference that moves with the distributor or to an absolute (fixed) system of reference.

The standard deviation of the temporal evolution of each PIV vector of solids relative velocity was obtained by means of Equation (7):

$$\sigma_{U_s} = \sqrt{\frac{1}{N}\sum_{i=1}^{N}(U_s(t) - U_{s,avg})^2} \tag{7}$$

where $U_{s,avg}$ is the time-averaged solids velocity in each window:

$$U_{s,avg} = \sum_{i=1}^{N} U_i(x, y)/N \tag{8}$$

4. Results and discussion

The results obtained in the present work are presented in three interrelated ways. Firstly, the oscillatory behavior of the bed bulk is studied by using the averaging of cycles method described in Section 3.2. Secondly, the PIV results concerning the bed solids oscillatory motion are analyzed altogether with their sensitivity to the static bed height, the vibration amplitude and the vibration frequency. Lastly, some results revealing the wave propagation phenomenon through the bed bulk are presented and discussed.

4.1. Oscillatory behavior of the bed bulk

Figure 2(a) shows a snapshot of the bed bulk at a time instant corresponding to an initial phase of the bed vessel oscillation $\phi \sim 0$ (i.e. the bed moving upwards and at its central position) for the base case (Exp. 1). The images depicted in Figure 2(b) and (d) show, respectively, a zoomed region of the bed surface and the bed bottom. Figure 2(b) shows the oscillation with time of the bed center of mass ($z = y_{cm,rel}$ in Equation (4)), surface position ($z = y_{fb}$) and the bed vessel position ($z = \delta$). The time increment between consecutive snapshots in Figure 2(b) and (d) is $\Delta t = 0.016$ s (i.e. every four recorded frames), which corresponds to an increment in phase of approximately $\Delta\phi \sim 0.275$ rad. The lines superimposed to the snapshots represent the oscillation of the bed surface (Figure 2(b)) and the bed vessel position (Figure 2(d)). It can be observed in Figure 2 that both the absolute position of the center of mass and the surface of the bed oscillate with a frequency equal to that of the bed vessel. Interestingly, the absolute position of the bed surface presents an oscillatory displacement in opposition of phase with the displacement of the bed vessel position. That means that when the bed vessel goes up the bed surface goes down and vice versa. Reversely, as shown in Figure 2(d), the bed vessel goes down when the bed surface goes up. This manifests a cyclic compression and expansion of the bed volume, similarly to the one encountered in other related experiments [16, 19, 34]. On the other hand, the absolute position of the center of mass of the bed oscillates with a phase equal to that of the bed vessel, as it is mainly affected by the oscillation of the whole bed bulk caused by the vessel vibration.

[Figure 2 about here.]

The oscillatory behavior of the surface and the center of mass of the bed can be further studied by means of the averaging of cycles method described in Section 3.2. Figure 3 shows the results concerning the absolute and relative positions of y_{fb} and y_{cm} as a function of the phase of the bed vessel ϕ and normalized with the vibration amplitude A. Recall that $\phi = 0$ corresponds to the beginning of a vibration cycle and $\phi = 2\pi$ to the end of the cycle. As in Figure 2, it can be observed in Figure 3 that both the absolute and the relative oscillations of y_{fb} present an opposition of phase with regard to the bed vessel oscillation. This indicates that the bed expansion and compression caused by vibration is larger than the oscillation of the

bed bulk. The origin of that may be attributed, in the expansion stage ($\phi = \pi/2 - 3\pi/2$), to the ease of the particles on the upper region of the bed bulk to maintain their upward velocity due to inertia despite the fact the bed bulk commences to descend. In addition, in the compression stage, the decrease of the bed bulk height ($\phi = 3\pi/2 - \pi/2$ of the next cycle) is larger than the bed vessel displacement. Figure 3 also shows the normalized bed volume, which is calculated with the instantaneous front area occupied by the bed particles in the image divided by WA, being W the bed width and A the vibration amplitude. Again, a cyclic compression and expansion of the bed volume in opposition in phase with the oscillation of the bed vessel is observed. As expected, the normalized oscillation of the bed volume is very close to that that of the relative position of the bed surface. The differences encountered between the two curves can be attributed to the slight changes in the bed volume caused by the separation of the bulk from the bed base (see Figure 2(d)), which takes place when the bed commences to descend ($\phi = \pi/2$).

[Figure 3 about here.]

4.2. Wave propagation in the bed

Figure 4 presents the results of the averaging of cycles of the absolute velocity vectors (Equation (5)) together with the contours of the solids velocity magnitude for the Experiment 1 (see Table 1). The velocity vectors and contours shown are averaged over intervals of $\Delta\phi = \pi/4$. As in Figure 3, ϕ represents the phase of the bed vessel displacement, with $\phi = 0 - \pi/2$ corresponding to the bed vessel moving upwards from the middle to the highest vertical position. It can be observed in the figure that the particles pertaining to the upper section of the bed (i.e. the bed volume close to the distributor) present absolute velocities that are different to those pertaining to the lower section of the bed (i.e. the bed volume close to the freeboard). When the particles in the upper section of the bed are moving up, the particles in the lower section are moving down and vice versa.

In Figure 4(f), the particles in the lower region of the bed have a downwards displacement, whereas in Figure 4(g) the particles move upwards in that region. This implies that the bed bulk impacts the bed vessel and the particle velocity changes in a phase close to $\phi = 3\pi/2$ which corresponds to the beginning of the ascending stroke of the bed vessel. Besides, in the phase interval $\phi = 3\pi/2 - 7\pi/4$ (Figure 4(g)) the particles belonging to the upper section of the bed maintain their descendant displacement, as the information of the impact of the bulk with the bed vessel has not arrived yet to the upper region of the bed.

Figure 4 has shown that the impact of the bed bulk with the base of the bed creates a disturbance that travels through the fluidized bed in the form of a wave. This is in harmony with the gas pressure wave reported by Wang et al. [33], on the basis of the same impact disturbance in a cylindrical vibrated fluidized bed. Therefore, it seems that the pressure wave is another manifestation of the velocity wave seen in Figure 4. The wave caused by the impact of the bed vessel with the distributor has a front horizontally extended

and travels upwards the bed bulk until it reaches the upper region of the bed around a phase $\phi \simeq \pi/4$ (of the next cycle). In that phase, the bed vessel commences to descend and, as the particles in the upper region of the bed still maintain their inertial displacement, two clearly distinguishable regions are formed in the bed in the phase interval $\phi = \pi/2 - 3\pi/4$. In the upper section of the bed particles move up and in the lower section of the bed the particles move down as a consequence of the descending motion of the bed vessel. In Figure 4(c-f) there exists an expansion wave in that travels upwards the bed and separates the bed in two regions of downward velocity of solids (close to the distributor) and upwards velocity of solids (in the upper section of the bed). In the phase interval $\phi = 3\pi/4 - \pi$ a small region of particles in the upper section of the bed still preserve their upward motion, which causes a smaller velocity of particles in the upper region in the subsequent phase intervals $\phi = \pi - 3\pi/2$. Again, in a phase around $3\pi/2$ the bed bulk impacts the distributor and the bulk behavior previously described is cyclically repeated.

[Figure 4 about here.]

In order to qualitatively study the propagation of the wave produced at the base of the bed, Figure 5 shows a detail of Figure 4 for a phase interval $\phi = 3\pi/2 - 2\pi$. This interval is decomposed in Figure 5 in small phase intervals of size $\Delta\phi = 0.0625\pi$. In Figure 5(a-b) it can be clearly observed the formation of a wave caused by the impact of the bed bulk with the distributor that propagates upwards in the bed. In Figure 5(b-h) the wave delimits two regions of upward and downward absolute velocity of solids in the bed bulk. Also, in Figure 5(b-c) the wave presents a "U" shape. This shape is caused because the wave generated on the distributor appears earlier close to the left and right corners than on the distributor center ($x = 0.15$ m). Near the corners, the friction of the particles with the lateral walls reduces the difference between the particles and the bed vessel velocities. This makes that the particles close to these corners impact the base of the bed with a smaller phase delay than the particles on the distributor center. When the wave is sufficiently far from the distributor (Figure 5 (c-h)) particles in the region under the wave present an upward velocity equal to the bed vessel ascending velocity as they are forced to move with the same velocity of the distributor. On the other hand, the particles above the wave present downward velocity and they cover a progressively smaller area.

[Figure 5 about here.]

Similarly to Figure 5, in Figure 6, the expansion wave generated in the vertically vibrated bed in the phase interval $\phi = \pi/2 - \pi$ was studied, which corresponds to a phase range of the expansion wave in which it can be clearly appreciated. This expansion wave clearly differentiates the bed bulk into two regions. One with an upward velocity of solids in the upper section of the bed bulk and other with a downward velocity of solids in the lower section of the bed. The formation of the expansion wave corresponds to the descending stroke of the bed vessel. In this phase interval, the bed vessel commences to move downwards

($\phi = \pi/2$) and the particles belonging to the lower section of the bed start to descend as they loose contact with the distributor. In Figure 6(c-d), a progressively larger volume of particles in the lower section of the bed is affected by this downward motion, which promotes the wave front to move upwards. However, particles belonging to the upper section of the bed remain their upward inertial displacement and cover a progressively smaller area in Figure 6(e-h).

[Figure 6 about here.]

Figure 7 shows the averaged (in the horizontal direction) normalized oscillation of the relative vertical velocity of solids along lines of constant absolute positions y situated at different heights from the distributor and as a function of the phase of the bed vessel. The horizontal lines in which the velocity is calculated are separated $\Delta y = 0.05$ m. The normalization is carried out by means of the bed vessel velocity, which was calculated using Equation (2), thus:

$$\overline{\Delta V}_s = \frac{\Delta V_s}{V} \tag{9}$$

In Figure 7, the oscillation of the solids velocity is larger as they are further from the distributor because they are more free to move due to the smaller mass of particles above them. This creates a delay of about π between the particles and the bed vessel velocities. Note that the relative velocity of the solids in the upper section of the bed, $y > 0.3$ m, is slightly larger than the velocity of the bed, $\overline{\Delta V}_s > 1$. This is attributed to the inertial displacement of the particles in the upper section of the bed when the bed vessel is moving downwards. In the lower region of the bed, the particles are more confined due to the weight of the bed bulk above them and that decreases the amplitude and delay of their velocity with respect to the vessel one. In addition, also in the lower region of the bed, the oscillation of the vertical velocity of solids follows a nearly sinusoidal displacement in the first half of the cycle $\phi = 0 - \pi$, which corresponds to the fraction of the cycle in which the bed vessel commences to decelerate and the velocity changes from positive to negative values. This creates a positive oscillation of the relative vertical velocity of the bed bulk, as particles maintain their upward velocity. In the second half of the cycle ($\phi = \pi - 2\pi$) the bed vessel velocity commences to increase from negative to positive values and that causes a decrease of the bed bulk relative velocity. As shown in Figure 5, the bed bulk impacts the distributor at a phase around $\phi \simeq 3\pi$ (4.7 rad). This is reflected in Figure 7 through the sudden increase of the oscillation of the vertical velocity of solids occurring at $\phi \simeq 5$ rad for the smaller distances from the distributor ($y = 0 - 0.2$ m). After impacting the distributor, the particles close to it adopt the vessel velocity, which leads to $\overline{\Delta V}_s = 0$ for $\phi > 5$ rad. The perturbation caused by the impact of the bed particles with the distributor is transmitted upwards with a finite velocity, as evidenced in Figure 7 with the progressive phase delay of the increase of $\overline{\Delta V}_s$ with y for $\phi > 5$ rad. Again, when the bed vessel commences to decelerate at $\phi = 0$, the oscillation of the bed relative velocity becomes greater

than zero and the whole process is cyclically repeated.

[Figure 7 about here.]

To quantitatively analyze the vertical distribution of the velocity wave, Figure 8 shows the evolution, for different time instants, of the solids velocity in the vertical direction. The solids velocity has been sampled from a vertical fringe of a width of $\Delta x \sim 0.02$ m (three PIV windows) situated in the central section of the bed ($x = W/2$) and also from two vertical fringes of the same width but close to the bed walls ($x = W/4$ and $x = 3W/4$). The velocity within each fringe is averaged horizontally to reduce noise. The figure shows a set of time instants separated $2\Delta t = 0.008$ s (i.e. $\Delta\phi = 0.86$ rad). The first time instant is t_0, which has a phase equal to $\phi = 0.08$ rad. It can be observed in Figure 8 that the behavior of the solids velocity in the different fringes along horizontal direction presents only a slight variation, which is caused by the non perfectly symmetrical impact of the bed bulk with the bed vessel, as seen in Figure 5. For $t = t_0$, the impact wave has already been generated at the bottom of the bed and the front of the velocity wave, which divides the bed in two regions with different relative velocities, is easily discernible. In $t = t_0 + 2\Delta t$, the bottom section of the bed presents a positive relative velocity, whereas there still exists a small region in the upper region of the bed in which particles are descending (in relative coordinates). In the subsequent time steps the relative velocity of the particles in all the bed bulk is positive and, when the bed commences to decelerate, it increases in the upper region of the bed. There is an instant, around $t = t_0 + 10\Delta t$ and $t = t_0 + 12\Delta t$, in which the bed bulk impacts the base of the bed and this cyclic behavior is repeated.

[Figure 8 about here.]

Considering that the bed presents a cyclic behavior, it could be of interest to study the behavior of solids and the wave propagation phenomenon in the bed as a function of the phase of the bed vessel. In this regard, Figure 9 presents the phase evolution of the solids velocity along a vertical fringe in the central section of the bed ($x = W/2$ and width $\Delta x \sim 0.02$ m). In Figure 9, every line averages the solids velocity pertaining to a phase $\phi = \phi_0 + i\Delta\phi$ ($i = 1, 2, ..., M$) along a complete experiment. In this case, $M = 32$ and $\Delta\phi = \pi/16$, which ensures the averaging of approximately 100 time instants for every phase interval. The results are normalized with the velocity of the bed vessel V.

Figure 9(a) shows the evolution of the relative particle velocity with the phase in a phase interval $\phi = 5.2 - 1.1$ rad (of the next cycle) as it represents the phase interval in which there is an upward compression wave inside the bed. It can be observed that, just before the bed bulk impacts the bed vessel, the whole bed bulk presents a net negative relative velocity ($\phi = 5.2$ rad in Figure 9(a)). From that phase interval on, the bed is clearly divided into two regions, which are separated by the compression wave front observed in Figure 5. One region with a relative vertical velocity of solids $V_s = 0$ as particles are being drifted upwards due to the presence of the base of the bed; and a region in which particles maintain their

negative relative velocity, as could be qualitative observed in Figure 5. There is a phase, around $\phi = 0.2$ rad in which the relative velocity of particles at the bottom of the bed is positive, which indicates that the bed bulk in that region is moving faster than the base of the bed, which is probably caused by the upward inertial velocity of the particles while the bed is decelerating.

Figure 9(b) represents the evolution of the particle velocity with the vibration phase in the phase interval $\phi = 1.3 - 5$ rad. There exist two clearly distinguishable subintervals of phase in Figure 9(b) concerning the behavior of the solids velocity. In the first one, marked in Figure 9 as "A", the relative velocity of the particles in the lower section of the bed scarcely varies whereas the bulk velocity in the upper section of the bed progressively increases. This corresponds to the fraction of the cycle in which the bed vessel commences to move downwards and the bed bulk detaches from the base of the bed. In the upper region of the bed, the particles maintain their inertial displacement and present a progressively larger upward velocity. At a phase close to $\phi = \pi/2$ the bed commences to expand as the relative velocity of the particles in the upper region of the bed is larger than in the lower region of the bed. Also, in Figure 9, the expansion wave described in Figure 6 commences to be observable in the subinterval "B" in Figure 9(b). In this subinterval, the particles in the whole bed bulk commence to reduce their velocity and the velocity in the upper region of the bed is larger than in the lower section of the bed, which promotes the expansion of the bed bulk observed in Figures 3 and 4. However, the upwardly advancing front of the expansion wave observed in "B" in Figure 9(b) is less pronounced as it produces a softer change in the relative vertical velocity of solids in the bed as the compression wave in Figure 9(a). As commented before, for a phase $\phi < 5$ rad, the bed bulk contacts the distributor and this cyclic behavior is repeated.

[Figure 9 about here.]

4.3. Effect of the static bed height

Figures 10 to 13 analyze the effect of the static bed height on the oscillatory behavior of the bed bulk and the wave propagation inside the bed. The amplitude of the vessel vibration, A, is similar in all the experiments of these figures. Firstly, similarly to Figure 3, the normalized oscillation of the bed surface and the bed center of mass is analyzed as a function of the vibration phase (see Figure 10) for different fill levels of the bed. It can be observed that the amplitude and phase of both the oscillation of the bed surface and the center of mass of the bed bulk remain practically unaffected regardless of the static bed height. This indicates that the oscillation of y_{fb} and y_{cm} are mainly caused by the bed vessel oscillatory displacement.

[Figure 10 about here.]

As in Figure 7, the effect of the static bed height on the oscillation of the relative velocity of particles as a function of the vibration phase at different heights y from the distributor is shown in Figure 11. For

the three static bed heights the oscillation of the bed bulk velocity presents a qualitative behavior similar to that described in Figure 7. However, quantitatively, the particles oscillate more vigorously (for the same distance to the distributor) when the static bed height is decreased. As in previous figures, this is attributed to the smaller amount of particles above the horizontal fringe of analysis, which permits particles to move more freely and with a larger velocity. For the same reason, the oscillation of the particle velocity presents a slightly larger delay when the static bed height is decreased. This is attributed to the ease of the bed vessel to lift a bed with a smaller volume of particles (i.e. smaller static bed height). If the volume of particles in the bed is smaller, the vibration of the bed vessel is able to fully detach the bed bulk from the distributor and create a larger gap than when volume of the bed is larger. This is so because less force is needed to lift the weight of particles in a bed of small static bed height due to both the smaller mass of the bed bulk and the more reduced friction with the vessel walls. This ultimately promotes an earlier impact of the bed with the larger static bed height, as observed in Figure 11 in the interval $\phi \sim 4.5 - 5.5$ rad.

[Figure 11 about here.]

To study the possible effect that the static bed height may have on the oscillation of the bed bulk and the regions of different oscillation velocities in the bed, Figure 12 shows the contour maps of the normalized standard deviation of the velocity of particles in the bed for the three static bed heights tested (see Section 3.3). Here, the standard deviation of the solids velocity is normalized with the bed velocity as shown in Equation (10).

$$\overline{\sigma}_{U_s} = \frac{\sigma_{U_s}}{V} \tag{10}$$

It can be observed in Figure 12 that the behavior of the bed is similar for the three experiments. That is, when H_0 is decreased, in the upper section of the bed the contour maps present a progressively larger standard deviation of the velocity due to the larger oscillation of particles when they have a smaller mass of solids above them. It is clear from Figure 12 that, in average, the velocity of the particles in the upper section of the bed oscillates more than in the lower section. This can explain why previous studies [16, 19, 26] have observed a change of bubble characteristics when passing from the lower to the upper sections of the bed. Noticeably, the upper section in which the particles oscillates more vigorously covers a slightly larger volume as the static bed height is increased. This suggests that the behavior of bubbles rising in a vibrated fluidized bed may differ depending on the static bed height and the position of the bubble in the bed.

[Figure 12 about here.]

The effect of the static bed height on the variation of the solids velocity in phase intervals of $\Delta\phi = \pi/16$ and along the bed height is studied in Figure 13 in a phase range $\phi = 0 - \pi$ (Figure 13(a)) and $\phi = \pi - 2\pi$

(Figure 13(b)). For simplicity, results of each $\Delta\phi = \pi/8$ are shown in Figure 13. The two regions in which the bed bulk is divided by the compression wave propagation along the bed height can be easily distinguished in Figure 13(a) in the phases in which the relative velocity of the solids in the lower section of the bed is close to zero and is negative in the upper section of the bed. Although in a lower extent, the expansion wave generated by the expansion of the bed bulk is also observable in the last phases of Figure 13(a) and in Figure 13(b), and it divides the bed bulk into two regions of smaller (lower section) and greater (upper section) relative vertical velocity of solids. In Figure 13(a), the compression wave in the bed with the smaller static bed height is ahead of the compression waves in the bed with larger H_0 because, in the former bed, the two regions of the different relative solids velocity have a smaller volume. However, no significant qualitative differences of the behavior of the bed bulk are encountered for the different H_0/W under study. In all the cases tested, the bed compresses and expands cyclically due to the different relative velocities of solids in the upper and lower sections of the bed.

[Figure 13 about here.]

4.4. Effect of the vibration amplitude and frequency

Figure 14 studies the effect of the vibration amplitude and frequency on the oscillatory behavior of the relative velocity of the particles of the bed bulk on horizontal lines at different distances from the distributor. Three different vertical coordinates are chosen in Figure 14: $y = 0.1$ m above the distributor, $y = 0.25$ m and $y = 0.35$ m (i.e. a distance of 0.1 m to the static bed height). Figure 14(a) shows that the normalized oscillation of V_s increases accordingly with A (i.e. $\Delta V_s = A \cdot \overline{\Delta V}_s$). The only remarkable difference encountered in Figure 14(a) among the different vibration amplitudes tested is found close to the distributor ($y = 0.1$ m). In that region, the phase ϕ in which the bed bulk impacts the distributor has a large influence on the phase delay of the solids in the lower section of the bed.

As for the variation of the vibration amplitude, the effect of the vibration frequency on the oscillation of the normalized relative particle velocity (Figure 14(b)) is also weak. In particular, prior to the impact of the bed vessel with the bed bulk, the oscillation of the normalized relative velocity of the particles in the lower region of the bed is smaller for smaller frequencies ($f = 13.9$ Hz) than for larger frequencies. The increase of the bed velocity caused by the increase of the vibration frequency affects slightly more the velocity of the particles inside the bed, contrary to the variation of the vibration amplitude in Figure 14(a). Note that, if the vibration frequency increases, the vibration strength, Λ, increases by a square factor, which makes the particles to be subjected to a larger acceleration. This is more noticeable in the lower sections of the bed, where the motion of particles is directly driven by the acceleration of the bed vessel.

[Figure 14 about here.]

Figure 15 shows the normalized standard deviation contour maps obtained for different vibration amplitudes (Experiments 1, 2 and 3 in Figure 15(a-c)) and the vibration frequency (Experiments 1, 4 and 5 in Figure 15(d-f)). As in Section 4.3, the standard deviation of the solids velocity was normalized with the bed vessel velocity by means of Equation (10). As in Figure 12, the standard deviation delimits two regions in the bed: an upper region, $y > 0.2$ m and a lower region $y < 0.2$ m. In all the cases, the upper region has the largest values of the normalized standard deviation (i.e. the bed velocity oscillates more vigorously). As commented previously, the particles belonging to the upper region of the bed oscillate more vigorously as they are less confined by the weight of the bed. Also, Figure 15 indicates that the volume of the two regions is independent of both the vibration amplitude and frequency. Counteracting effects of the vibration amplitude and frequency seem to be affecting the behavior of the particles in the lower region of the bed, where the normalized oscillation of the particle velocity is smaller. When increasing the vibration frequency in Figure 15(a-c), the normalized standard deviation of the particle velocity in the lower region of the bed slightly increases, which is probably due to a higher average voidage in the lower section promoted by the increase of the vibration frequency, which allows for the particles to move more freely. On the contrary, when increasing the vibration amplitude in Figures 15 (c-e), $\overline{\sigma}_{U_s}$ slightly decreases for $y \lesssim 0.05$ m. This indicates that the oscillation of the particle velocity in the lower region of the bed might be damped by large amplitudes of vibration that densely pack the bed in that region and impede the particle movement.

[Figure 15 about here.]

The effect of the vibration frequency and amplitude on the phase variation of the normalized vertical velocity of solids in a vertical stripe of width $\Delta x = 0.02$ m situated in the middle of the bed is depicted in Figure 16. As in Figure 13, phase intervals of $\Delta\phi = \pi/16$ with phase steps of $\Delta\phi = \pi/8$ within the different curves in Figure 16 were chosen. Figures 16(a,c) show the results of the phase intervals belonging to $\phi = 0 - \pi$, whereas Figures 16(b,d) depict results within the range $\phi = \pi - 2\pi$. The effect of the different vibration amplitudes on the normalized solids velocity can be appreciated in the first phases of the wave propagation in the bed in Figure 16(b), $\phi = 5.01 - 6.19$ rad. The compression wave of velocity generated for $A = 4.1$ mm is slightly forward in phase with respect to the cases of $A = 4.7$ mm and $A = 5.2$ mm. This is probably caused by the higher distance the bed lifts from the distributor when increasing the vibration amplitude, which delays (in phase) the impact of the bed vessel and the bed bulk. The effect of the vibration frequency on the normalized vertical velocity of solids is shown in Figure 16(c-d). Here, the lines corresponding to the different vibration frequencies are nearly overlapped except in the phase intervals in which the wave is in the lower region of the bed ($\phi = 5.01 - 6.19$ rad of Figure 16(d)). From all this, it can be extracted that the mechanism of wave propagation and the normalized velocity profiles of solids in the bed appears to be slightly affected of the vibration amplitude and frequency in the present range of conditions studied. This means that the amplitude of the velocity wave depends directly on the velocity of

the bed vessel; that is, if the normalization of the velocity is undone, it is nearly proportional to A and f^2.

[Figure 16 about here.]

4.5. Wave propagation velocity

As commented in the previous sections, the results show that there exists a compression wave that is generated at the bottom of the bed vessel and travels inside the bed. There is also an expansion wave going upwards. Thus, it would be interesting to characterize the velocity at which the velocity waves travel inside the bed bulk. Only compression waves will be studied in this section as they are more intense and easier to analyze.

Firstly, the instantaneous position of the front of a compression wave of velocity of the particles inside the bed was obtained by means of the averaging of cycles method for the absolute vertical velocity of the particles in the bed (similarly as in Figure 9). In this case, the absolute velocity of particles was discretized in $M = 64$ phase intervals in order to have a sufficient number of phase points in which the wave position was determined without compromising the statistical accuracy of the results. The wave vertical position was calculated as the vertical coordinate, in a vertical stripe of $\Delta x \sim 0.02$ m in the center of the bed, at which the absolute vertical velocity of the particles is equal to a threshold value that separates the maximum to the minimum vertical velocity of solids in the wave. This threshold is taken equal to half the maximum vertical velocity of solids in the vertical stripe. As the bed impacts the bed vessel in a phase $\phi \sim 3\pi/2$, the wave position is calculated in an interval starting at $\phi = 3\pi/2$ and ending at $\phi = 7\pi/2$ (i.e. $\pi/2$ of the next cycle), which corresponds to the whole ascending stroke of the bed vessel.

Figure 17(a) shows the evolution of the position of the front of the velocity wave as a function of the vibration phase for the different experiments listed in Table 1. Two clearly distinguishable regions are observed. In the lower section of the bed ($y < 0.2$ m), a fast increase of the wave front position appears, which is attributed to the more efficient wave transmission due to the denser packing of particles in this lower section of the bed. When the wave is sufficiently far from the distributor ($y > 0.2$ m), the position of the wave front increases less rapidly and more linearly. Comparison of the different experiments depicted in Figure 17 shows that a similar trend is followed by the evolution of the wave position regardless the vibration amplitude and frequency of the bed.

Reducing the static bed height for the same vibration conditions in Figure 17(a) seems to reduce the region in which the wave position presents a fast increase. Also, the front of the compression waves present in the bed filled with a smaller H_0/W travels slower than in beds filled with a larger static bed height. This is probably associated to the larger confinement of particles in the lower region of the bed for larger H_0/W, which allows for a faster traveling of the perturbation along the bed [30].

The velocity of propagation of the wave inside the bed was calculated by means of Equation (11).

$$V_{prop} = \left(\frac{\omega \Delta y}{\Delta \phi} \right) \tag{11}$$

where $\omega = 2\pi f$ is the angular frequency of vibration and Δy and $\Delta \phi$ denote, respectively, the variation of the absolute vertical position and the phase interval between two consecutive positions of the wave front in Figure 17(b)

Figure 17(b) presents the results of the wave propagation velocity calculated by means of Equation (11). The wave propagation velocity shows a maximum value when the wave is close to the distributor ($y < 0.2$ m), which corresponds to the larger slope of the wave position in Figure 17(a). According to Figure 17(b), the maximum wave velocity increases when the vibration amplitude and frequency are augmented. This observation suggests that, right after being generated, the wave propagation velocity is directly affected by the bed vessel acceleration, which densely packs the lower section of the bed, promoting a faster wave front. After this maximum value, V_{prop} progressively decreases and remains in the range $V_{prop} = 5 - 10$ m/s for all the experiments. This progressive decrease of V_{prop} may be caused by the progressively increasing voidage of the bed bulk as the wave front travels upwards. This is probably caused by the smaller confinement of particles in the upper region of the bed (see Section 4.2) where the wave propagation velocity decreases because the bed is less densely packed [30].

[Figure 17 about here.]

To see the sensitivity of the compression wave velocity on the acceleration of the bed, Figure 18 shows the mean, median and maximum value of the results of V_{prop} shown in Figure 17(b). The results in Figure 18 are represented as a function of the vibration strength for the experiments with the same bed heights. It is clear from the figure that when Λ is increased, the mean velocity of the wave and, especially, the median, are weakly affected because these velocities are principally affected by the numerous data of wave propagation far from the distributor ($\phi > 6$ in Figure 17(b)) and less by the wave propagation data close to the distributor ($\phi < 6$). In contrast, the standard deviation and the maximum velocity of the compression wave grow with Λ, in correspondence with the dispersion of data with A and f in Figure 17(b) that is only important for $\phi < 6$.

In general, the mean and median values of the wave propagation velocity in the vibrated fluidized bed are in accordance to the classical values of the sound propagation velocity in a fluidized bed [30]. These values are also in harmony with previous works in which the wave propagation velocity was calculated by means of the delay of the perturbation that vibration causes in the oscillation of bubble characteristics [19, 26]. Alternatively, in [23] the pressure wave propagation velocity is calculated in a vibrated fluidized bed as a function of the vibration frequency in a bed in bubbling regime. They observed that the propagation velocity increased with the vibration frequency. However, for the particles and the range of vibration amplitudes

and frequencies tested in the present work, the wave propagation velocity presented a small variation with the vibration frequency. All these results show that, once the bed bulk impacts the base of the bed and the compression wave is generated, it travels in the bed at a velocity that is weakly affected by the vibrating conditions (e.g. Λ), excepting for a region close to the distributor.

[Figure 18 about here.]

5. Conclusions

The oscillatory behavior of the bed bulk and the particles in a vertically vibrated fluidized bed were experimentally studied in the present work by means of DIA and PIV. Experiments comprising beds of Geldart B particles aerated at minimum fluidization velocity and with different static bed heights and vibration amplitudes and frequencies were carried out. An averaging of cycles methodology was employed for the analysis of the oscillation of the surface and the center of mass of the bed as well as for the characterization of the periodic distribution of the solids velocity.

The results showed that the bed presents a cyclic compression and expansion caused by the vibration of the bed vessel. Analysis of the PIV results revealed that there exists a compression wave of solids velocity that spans the whole bed width. This wave is generated by the impact of the bed bulk with the gas distributor and travels upwards dividing the bed into two regions with different relative velocities. That is, the particles under the wave move upwards and the particles above the wave move downwards. It was also found that during the expansion phase of the bed, a less intense wave appears and travels upwards with particles under the wave moving downwards and particles above the wave moving upwards.

The effects of the static bed height and the vibration amplitude and frequency on the oscillation and the velocity wave propagation were also studied. When the static bed height is increased the spatial distribution of the oscillation of solids velocity presents the same qualitative behavior. However, the amplitude of the oscillation of the solids velocity at a given vertical position decreases because the column of particles above this position augments when the bed height is increased. The vibration amplitude changes proportionally to the amplitude of the oscillation of the particle velocity in the bed. An increase of the vibration frequency increases the amplitude of the solids velocity oscillation. Close to the distributor of the bed, the wave velocity presents a maximum which is directly produced by the upward displacement of the gas distributor in cooperation with the dense packing of particles in that region during the compression phase of the vibration cycle. Far from the distributor, the wave velocity reaches values between 5 to 10 m/s approximately, which are nearly independent of the vibration frequency, amplitude and the static bed height.

All the previously presented results help to shed light onto the different behaviors of bubbles and pressure signals reported in previous works regarding vibrating fluidized beds. The oscillation of the bed bulk and

the propagation of velocity waves here analyzed can help to understand the fundamental mechanisms of particle-vessel interaction and the bubble behavior in vibrated fluidized beds.

Nomenclature

A = vibration amplitude (mm)

f = vibration frequency (Hz)

g = gravity acceleration constant (m/s^2)

H = bed height (m)

H_0 = static bed height (m)

K = bed thickness (m)

M = number of phase intervals for averaging of cycles (-)

N = number of frames in an experiment (-)

t = time (s)

T = period of vibration (s)

U_{mf} = minimum fluidization velocity (m/s)

U_s = solids velocity (m/s)

$v(t)$ = bed vessel instantaneous velocity (m/s)

V = bed vessel velocity (m/s)

V_{prop} = wave front propagation velocity (m/s)

V_s = solids vertical velocity (m/s)

$\overline{V}_s$ = normalized solids vertical velocity (m/s)

W = bed width (m)

x = horizontal coordinate (m)

y = vertical coordinate (m)

y_{fb} = bed surface vertical coordinate (m)

y_{cm} = bed center of mass vertical coordinate (m)

y_w = wave front vertical coordinate (m)

$z(t)$ = instantaneous variable value

$\widehat{z}(t)$ = moving average of z

Greek letters

Λ = vibration strength (-)

$\delta(t)$ = instantaneous vibration displacement (m)

ϕ = bed vessel vibration phase (rad)

ω = angular frequency (rad/s)

Acknowledgments

This work has been partially funded by the Spanish Ministry of Economy and Competitiveness (project ENE2015/00188/001).

References

[1] D. Kunii, O. Levenspiel, Fluidization Engineering, Butterworth-Heinemann, Newton, MA, 1991.

[2] W.C. Yang, Handbook of fluidization and fluid-particle systems, Marcel Dekker Inc. 2003.

[3] R. Gupta, A.S. Mujumdar, Aerodynamics of a vibrated fluid bed, Can. J. Chem. Eng. 58 (1980) 332-338.

[4] C. Strumillo, Z. Pakowski, Drying of granular products in vibrofluidized beds, in: A.S. Mujumdar (Ed.), Drying'80: Developments in Drying, Hemisphere Publishing Corporation, Montreal, (1980) 211-226.

[5] A.S. Mujumbar, Handbook of Industrial Drying. Marcel Dekker. New York, 1987.

[6] N.J.M Kuipers, E.J. Stamhuis, A.A.C.M. Beenackers, Fluidization of potato starch in a stirred vibrated fluidized bed, Chem. Eng. Sci. 51 (1996) 2727-2732.

[7] Y. Mawatari, Y. Tatemoto, K. Noda, Prediction of minimum fluidization velocity for vibrated fluidized bed, Powder Technol. 131 (2003) 66-70.

[8] Y. Mawatari, M. Tsunekawa, Y. Tatemoto, K. Noda, Favorable vibrated fluidization conditions for cohesive fine particles, Powder Technol. 154 (2005a) 54-60.

[9] X. Yang, Y. Zhao, Z. Luo, S. Song, C. Duan, L. Dong, Fine coal dry cleaning using a vibrated gas-fluidized bed, Fuel Process. Technol. 106 (2013) 338-343.

[10] K. Noda, Y. Mawatari, S. Uchida, Flow patterns of fine particles in a vibrated fluidized bed under atmospheric or reduce pressure, Powder Technol. 99 (1998) 11-14.

[11] T. Zhou, H. Kage, S. Funaoka, H. Ogura, Y. Matsuno, Fluidization behaviour of glass beads under different vibration modules, Adv. Powder Technol. 12 (2001) 559-575.

[12] E.R.A. Eccles and A.S. Mujumdar, Bubble phenomena in aerated vibrated beds of small particles, Drying Technol. 15:1 (1997) 95-116.

[13] Y. Mawatari, K. Tagawa, Y. Tatemoto, K. Noda, Bubbling characteristics under vertical vibration in a two-dimensional fluidized bed, Chem. Eng. Jpn. 38 (2005b) 18-23.

[14] T. Zhou, H. Ogura, M. Yamamura, H. Kage Bubble motion pattern and rise velocity in two-dimensional horizontal and vertical vibro-fluidized beds, Can. J. Chem. Eng, 82 (2004) 236-242.

[15] T. Zhou, H. Kage, H. Li, Bubble characteristics in a two-dimensional vertically vibro-fluidized bed, China Partic. 3 (2005) 224-228.

[16] E. Cano-Pleite, Y. Shimizu, F. Hernndez-Jimnez, A. Acosta-Iborra, Y. Mawatari, Effect of vertical vibration and particle size on the solids hold-up and mean bubble behavior in a pseudo-2D fluidized bed, Chem. Eng. J. 304 (2016) 384-398.

[17] J.A. Laverman, I. Roghair, M. van Sint Annaland, Kuipers, H., Investigation into the hydrodynamics of gas-solid fluidized beds using particle image velocimetry coupled with digital image analysis, Can. J. Chem. Eng. 86 (2008) 523-535.

[18] F. Hernández-Jiménez, S. Sánchez-Delgado, A. Gómez-García, A. Acosta-Iborra, Comparison between two-fluid model simulations and particle image analysis & velocimetry (PIV) results for a two-dimensional gas-solid fluidized bed, Chem. Eng. Sci. 66 (2011) 3753-3772.

[19] E. Cano-Pleite, F. Hernández-Jiménez, M. de Vega, A. Acosta-Iborra, Experimental study on the motion of isolated bubbles in a vertically vibrated fluidized bed, Chem. Eng. J., 255 (2014) 114-125.

[20] D. Santana, S. Nauri, A. Acosta, N. Garca, A. Macas-Machn, Initial particle velocity spatial distribution from 2-D erupting bubbles in fluidized bed, Powder Technol. 150 (2005), 1-8.

[21] C. Zeilstra, M.A. van der Hoef, J.A.M. Kuipers, Experimental and numerical study of solids circulation in gas-vibro fluidized beds, Powder Technol. 248 (2013) 153-160.

[22] Y. Tatemoto, Y. Mawatari, T. Yasukawa, K. Noda, Numerical simulation of particle motion in vibrated fluidized bed, Chem. Eng. Sci. 59 (2004) 437-447.

[23] L. Xiang, W. Shuyan, L. Huilin, L. Goudong, C. Juhui, L. Yikun, Numerical simulation of particle motion in vibrated fluidized beds, Powder Technol. 197 (2010) 25-35.

[24] S. Limtrakul, W. Rotjanavijit, T. Vatanatham, Lagrangian modeling and simulation of effect of vibration on cohesive particle movement in a fluidized bed, Chem. Eng. Sci. 62 (2007) 232-245.

[25] A. Acosta-Iborra, F. Hernández-Jiménez, M. de Vega, J.V. Briongos, A novel metodology for simulating vibrated fluidized beds using two-fluid models, Chem. Eng. J. 198-199 (2012) 261-274.

[26] E. Cano-Pleite, F. Hernndez-Jimnez, A. Acosta-Iborra, Compressible-gas two-fluid modeling of isolated bubbles in a vertically vibrated fluidized bed and comparison with experiments, Chem. Eng. J. 271 (2015) 287-299.

[27] R. Roy, J.F. Davidson, V.G Tuponogov, The velocity of sound in fludised beds, Chem. Eng. Sci. 45 (1990) 3233-3245.

[28] D. Musmarra, M. Poletto, S. Vaccaro, R. Clift, Dynamic waves in fluidized beds, Powder Technol. 82 (1995) 255-268.

[29] J. van der Schaaf, J.C. Schouten, C.M. van den Bleek, Origin, propagation and attenuation of pressure waves in gas-solid fluidized beds, Powder Technol. 95 (1998) 220-233.

[30] Hsiaotao T. Bi, A critical review of the complex pressure fluctuation phenomenon in gas-solids fluidized beds, Chem. Eng. Sci. 62 (2007)3473-3493.

[31] S. Sasic, B. Leckner, F. Johnsson, Characterization of fluid dynamics of fluidized beds by analysis of pressure fluctuations, Prog. Energy Combust. Sci. 33 (2007) 453-496.

[32] T. Wang, Y. Jin, Z. Wang, Z. Yu, The characteristics of wave propagation in a vibrating fluidized bed, Chem. Eng. Technol. 20 (1997) 606-611.

[33] T.J. Wang, Y. Jin, A. Tsutsumi, Z. Wang, Z. Cui, Energy transfer mechanism in a vibrating fluidized bed, Chem. Eng. J. 78 (2000) 115-123.

[34] D. Barletta, P. Russo, M. Poletto, Dynamic response of a vibrated fluidized bed of fine and cohesive powders, Powder Technol. 237 (2013) 276-285.

[35] D. Geldart, Types of gas fluidization, Powder Technol. 7 (1973) 285.
Evaluation of minimum fluidizing velocity in gas fluidized bed from pressure fluctuations (1985) Chemical Engineering Communications, 35 (1-6), pp. 81-87.

[36] N. Otsu, A threshold selection method from gray-level histograms, IEEE Transactions on Systems, Man and Cybernetics, 9 (1979) 62-66.

[37] J.K. Sveen, MATPIV, 1998-2014, https://www.mn.uio.no/math/ /people/aca/jks/matpiv/.

List of Figures

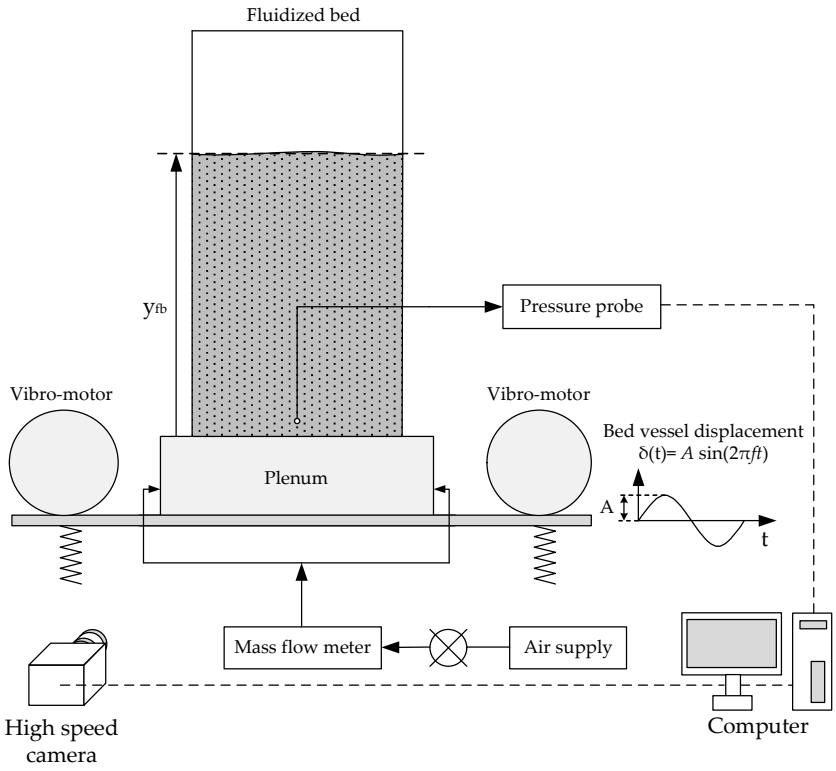

Figure 1: Sketch of the experimental facility.

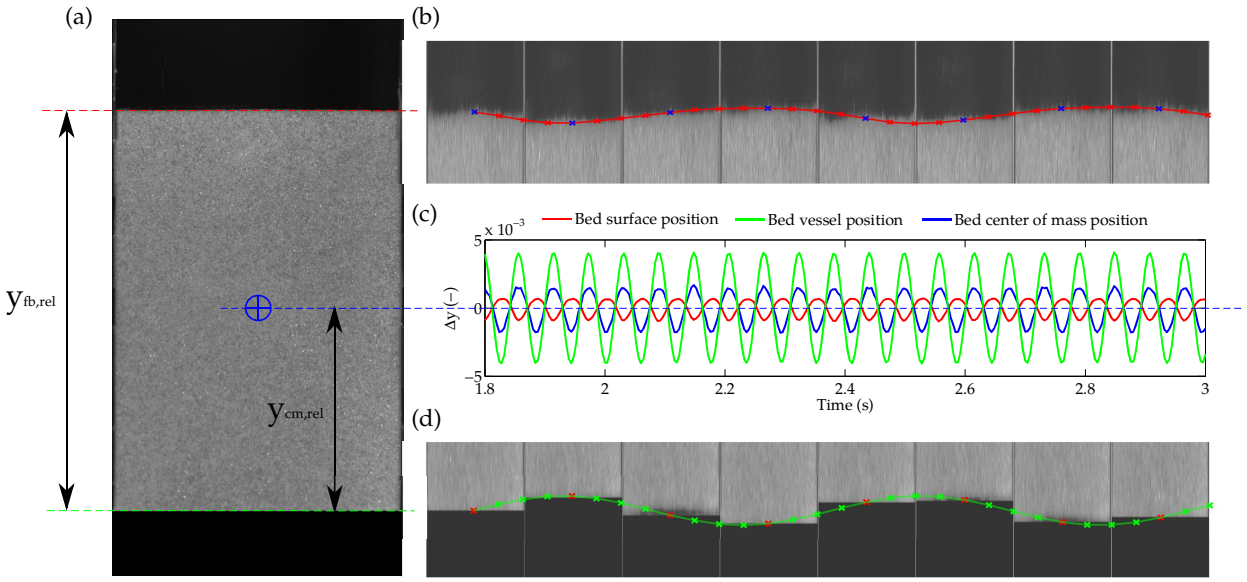

Figure 2: Oscillation of the bed bulk at minimum fluidization. (a) Snapshot of the bed taken by the high speed camera. (b) Zoomed snapshots of the bed surface superimposed by the oscillation of the bed surface. (c) Evolution with time of the oscillation of the bed surface, the bed position and the bed center of mass. (d) Zoomed snapshots of the bed base position superimposed by the oscillation of the bed position. Experiment 1.

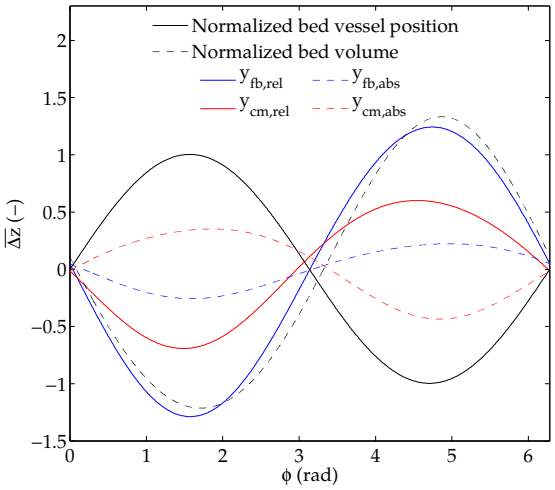

Figure 3: Oscillation of the bed vessel position, the bed volume and the absolute and relative positions of the freeboard and the center of mass of the bed. Experiment 1.

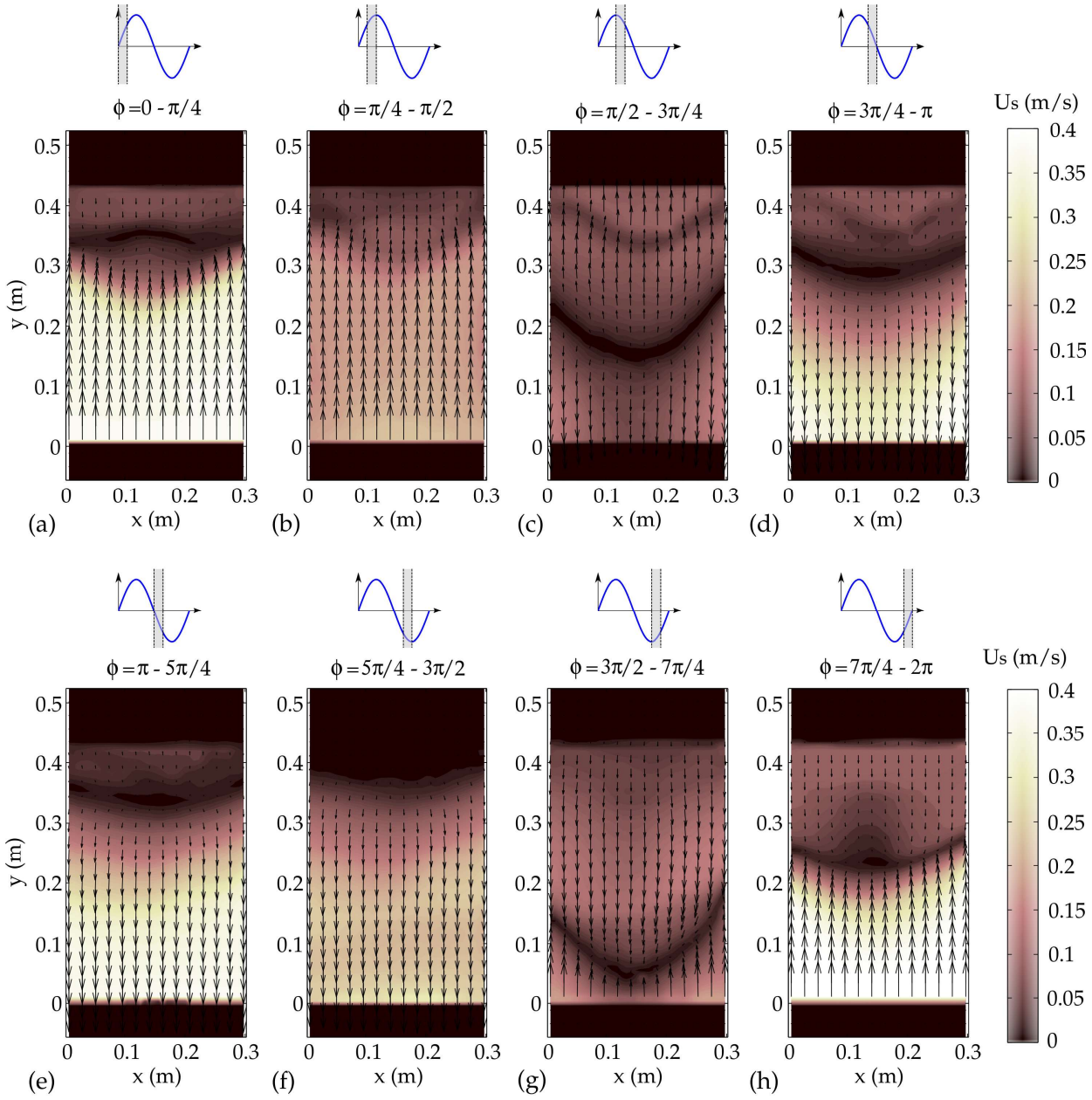

Figure 4: Averaging of cycles of the absolute velocity of solids in the vertically vibrated fluidized bed for eight different phase intervals of size $\Delta\phi = \pi/4$ over a total interval $\phi = 0 - 2\pi$. The velocity vectors are shown superimposed to the velocity magnitude contours. Experiment 1.

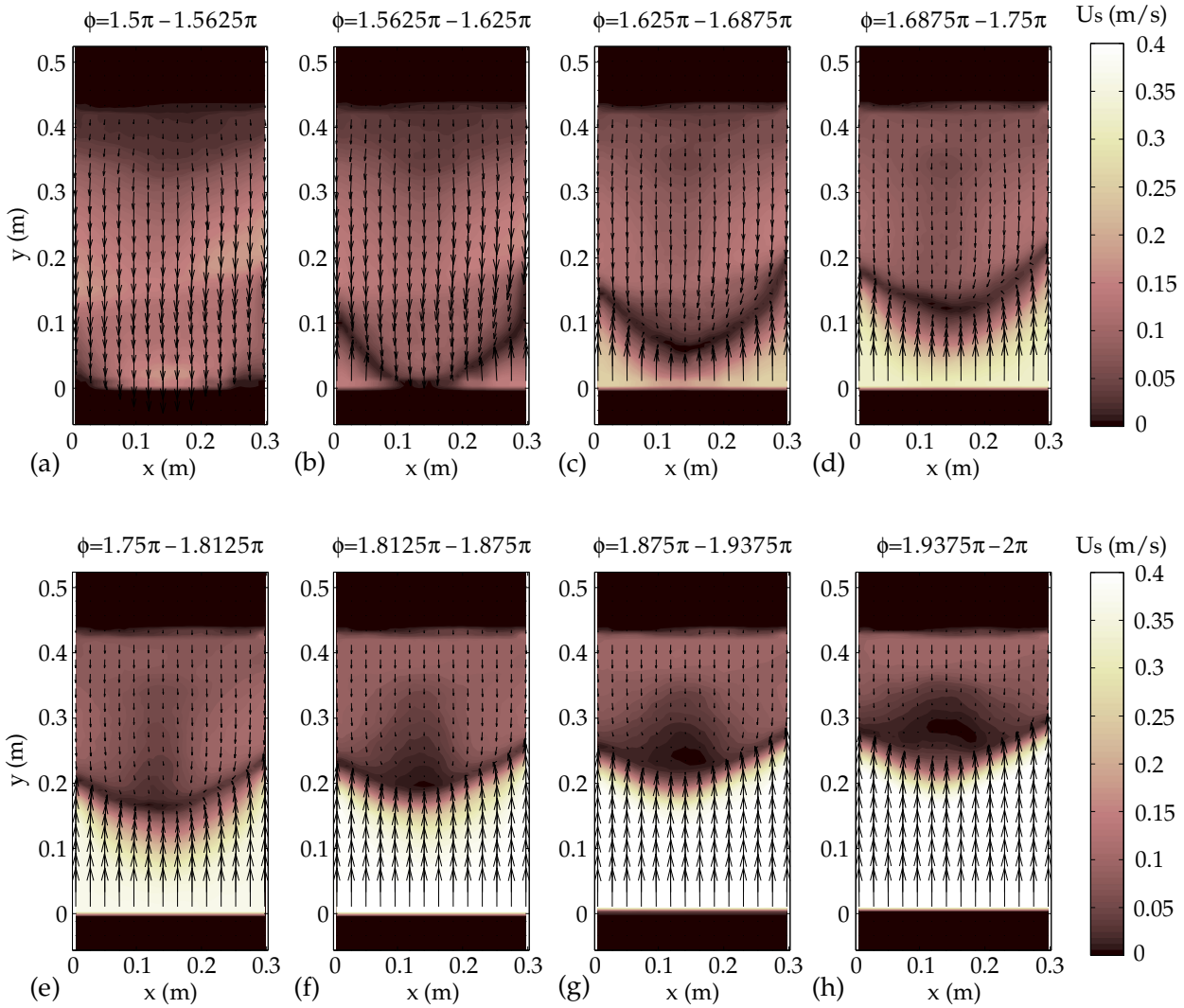

Figure 5: Averaging of cycles of the absolute velocity of solids in the vertically vibrated fluidized bed for eight different phase intervals of size $\Delta\phi = \pi/16$ over a total interval $\phi = 1.5\pi - 2\pi$. The velocity vectors are shown superimposed to the velocity magnitude contours. Experiment 1.

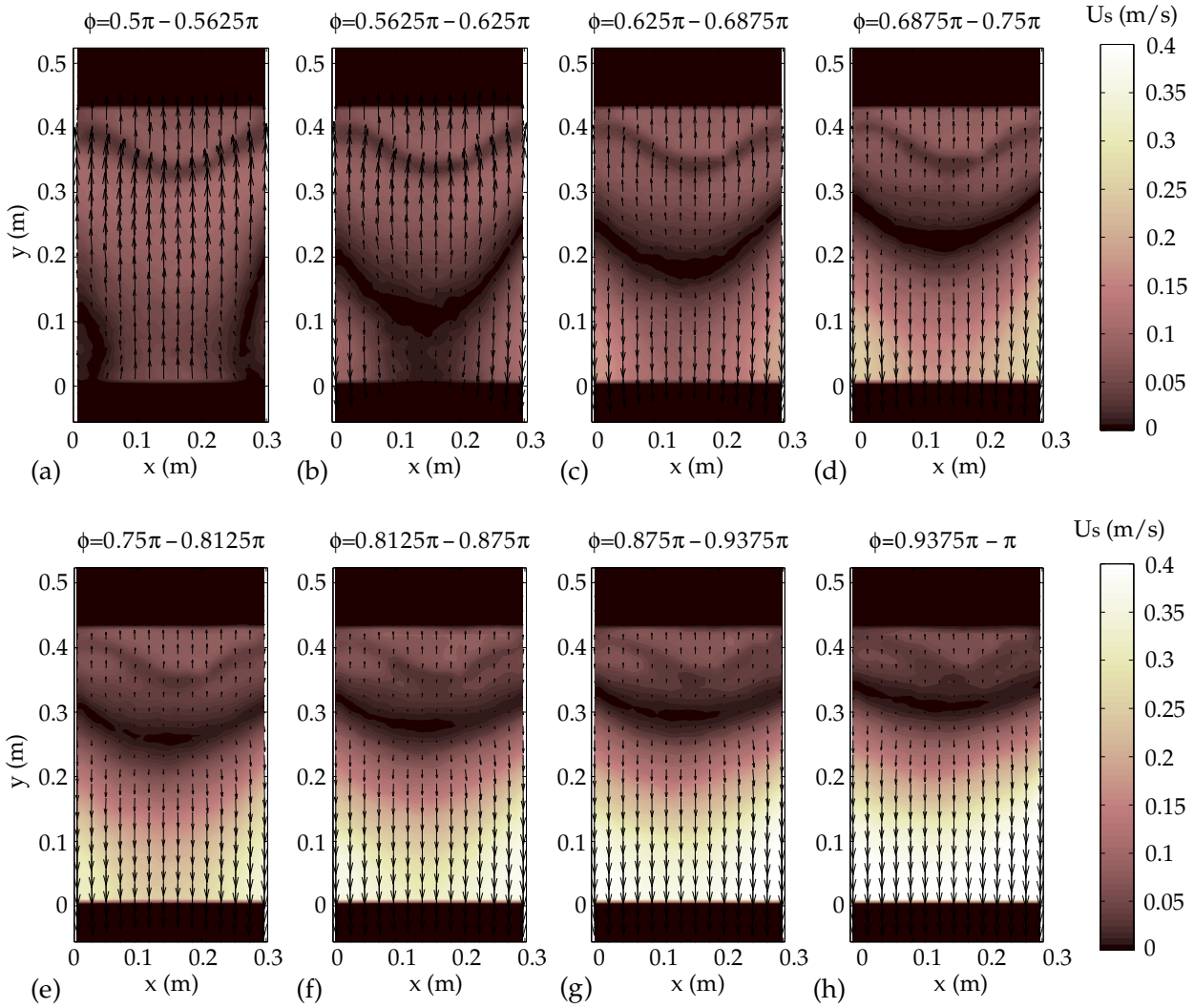

Figure 6: Averaging of cycles of the absolute velocity of solids in the vertically vibrated fluidized bed for eight different phase intervals of size $\Delta\phi = \pi/16$ over a total interval $\phi = 0.5\pi - \pi$. The velocity vectors are shown superimposed to the velocity magnitude contours. Experiment 1.

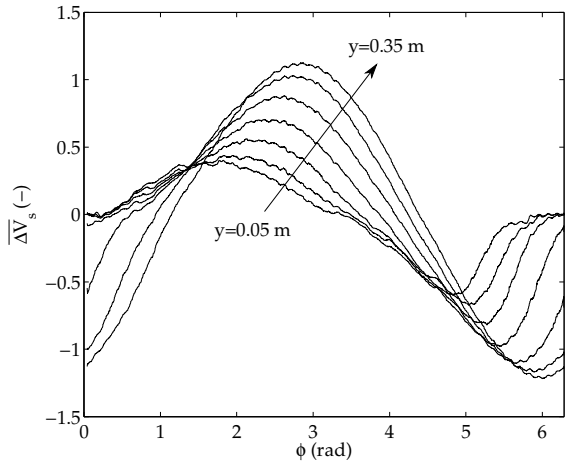

Figure 7: Oscillation of the normalized relative vertical velocity of solids at different distances from the distributor. The lines in which the particle velocity is calculated are separated $\Delta y = 0.05$ m. Experiment 1.

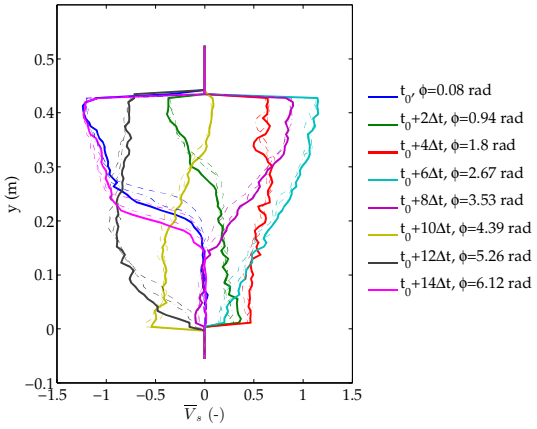

Figure 8: Time evolution of the relative vertical velocity of solids along the vertical direction. Solid line: vertical fringe at $x = W/2$. Dashed-dotted and dashed lines: vertical fringes situated at $x = W/4$ and $x = 3W/4$. Experiment 1.

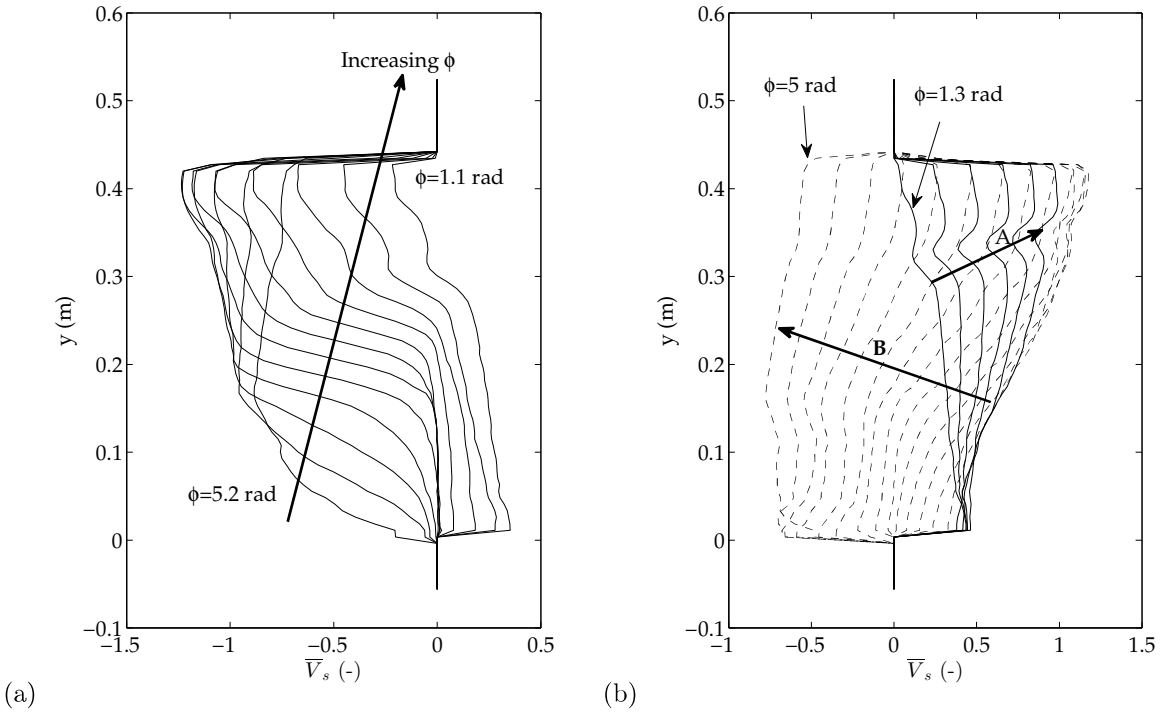

Figure 9: Vertical evolution of the normalized relative vertical velocity of the solids in the bed for different phase intervals: (a) Phase interval comprising the compression wave propagation in the bed, (b) Phase interval comprising the expansion of the bed bulk and the expansion wave propagation until the bed bulk impacts the distributor. Experiment 1.

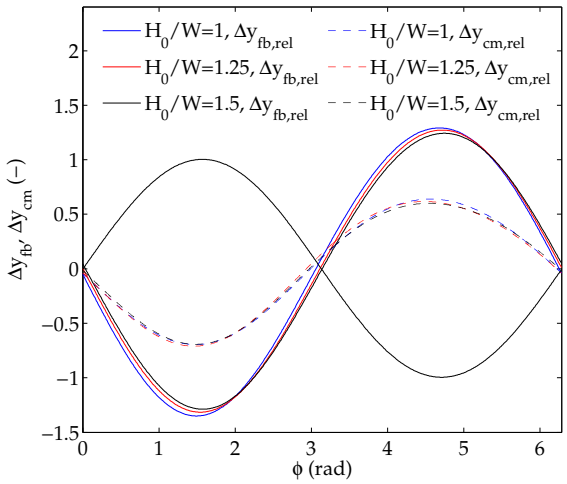

Figure 10: Effect of the static bed height on the oscillation of the bed vessel position and the absolute and relative positions of the freeboard and the center of mass of the bed. The solid black line indicates the normalized bed vessel position. Experiments 1, 6 and 7.

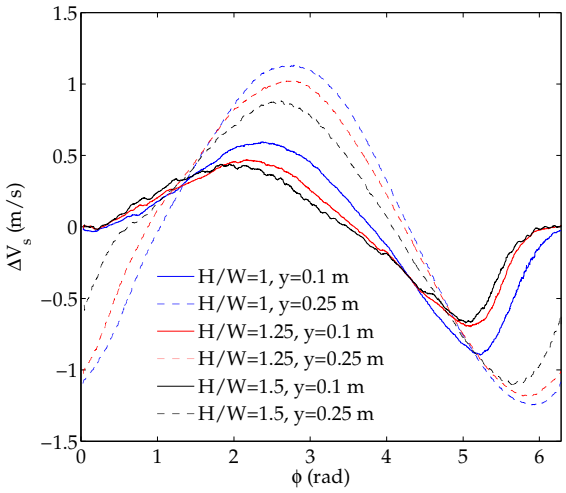

Figure 11: Effect of the static bed height on the oscillation of the normalized relative vertical velocity of solids at different distances from the distributor. Experiments 1, 6 and 7.

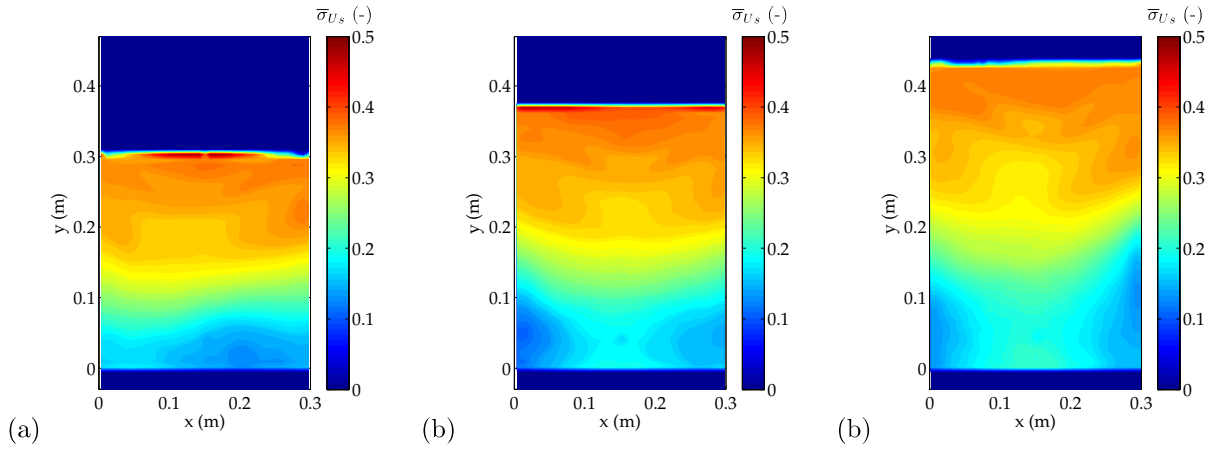

Figure 12: Effect of the static bed height on the normalized standard deviation contour map of the solids velocity: (a) $H_0/W = 1$, (b) $H_0/W = 1.25$ and (c) $H_0/W = 1.5$. Experiments 6, 7 and 1.

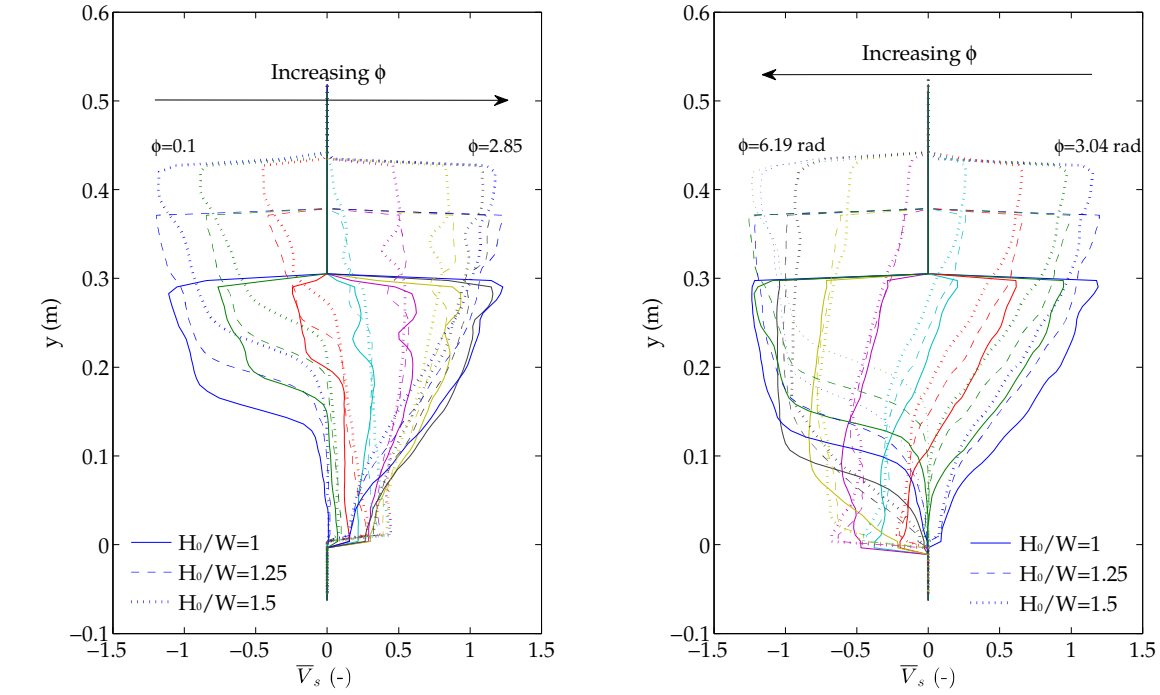

Figure 13: Vertical evolution of the normalized relative vertical velocity of the solids in the bed for different phase intervals and static bed heights. (a) $\phi = 0 - \pi$, (b) $\phi = \pi - 2\pi$. Experiments 1, 6 and 7.

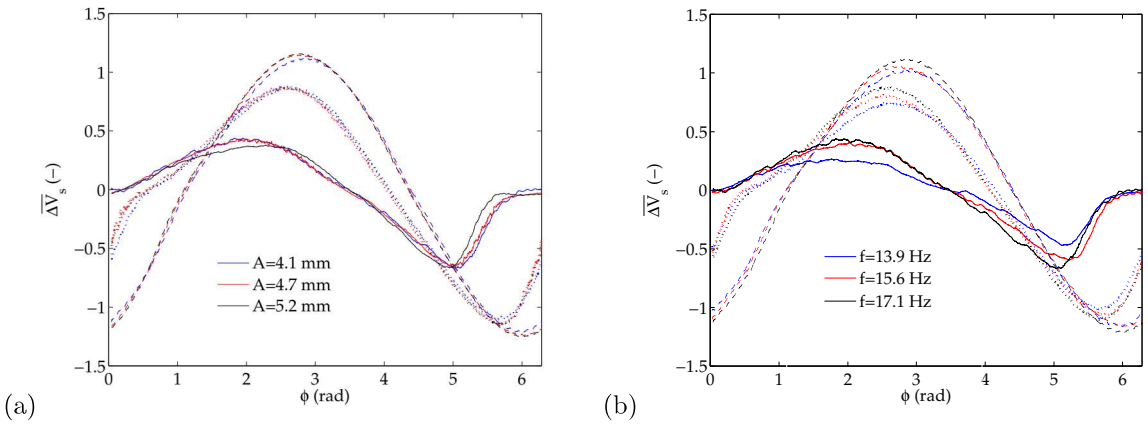

Figure 14: Normalized oscillation of the solids relative vertical velocity at different distances from the distributor. Solid lines: $y = 0.1$ m. Dotted lines: $y = 0.25$ m. Dashed lines $y = 0.35$ m. (a) Variation with the vibration amplitude (Experiments 1, 2 and 3), (b) variation with the vibration frequency. (Experiments 1, 4 and 5).

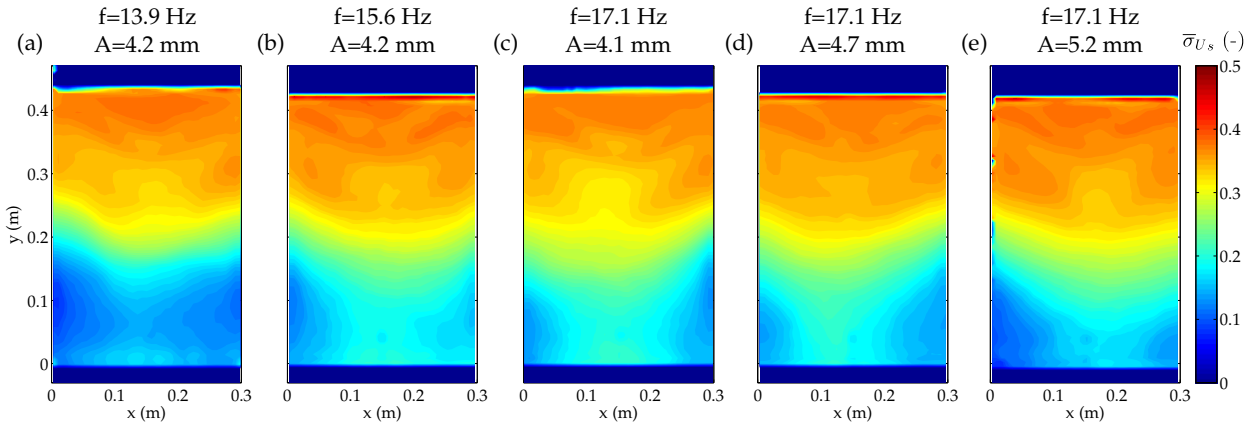

Figure 15: Normalized standard deviation contour map of the velocity of solids. (a-c) Variation with the vibration frequency (Experiments 4, 5 and 1), (c-e) variation with the vibration amplitude (Experiments 1, 2 and 3).

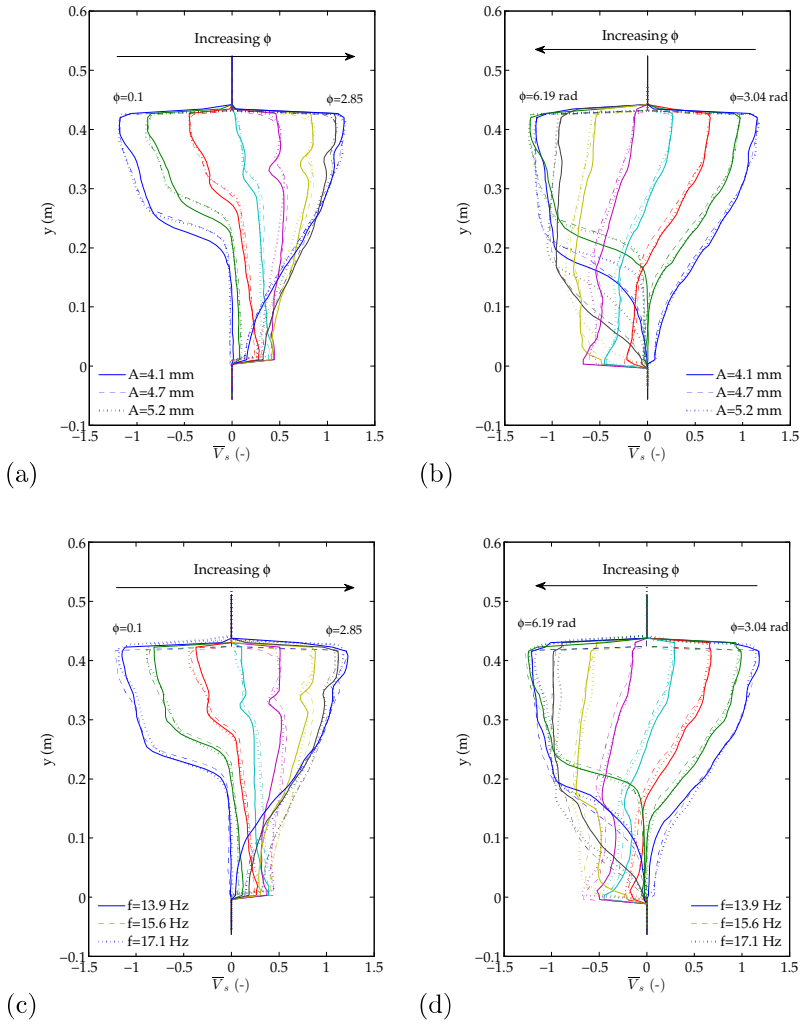

Figure 16: Vertical evolution of the normalized vertical velocity of the solids in the bed for different phase intervals. (a-b) Effect of the vibration amplitude (Exp. 1, 2 and 3). (c-d) Effect of the vibration frequency (Exp. 1, 4 and 5). (a,c) Phase interval $\phi = 0 - \pi$, (b,d) phase interval $\phi = \pi - 2\pi$.

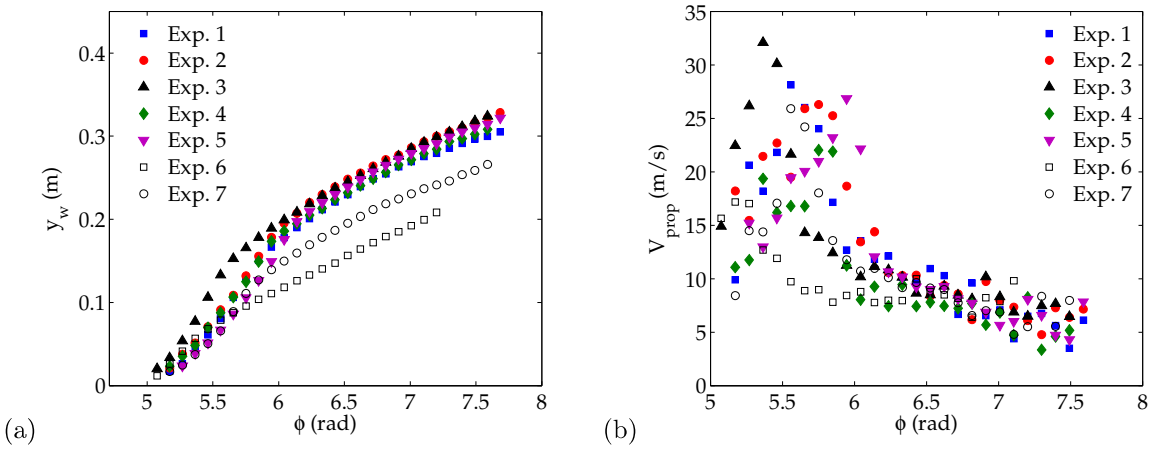

Figure 17: Evolution of the compression wave position (a) and velocity (b) as a function of the vibration phase.

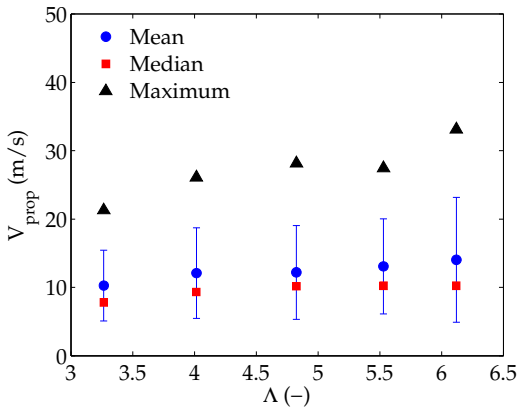

Figure 18: Mean, median, maximum and standard deviation of the wave absolute propagation velocity in the bed as a function of the vibration strength Λ. Experiments 1-5.

List of Tables

Table 1: Experimental conditions.

Exp.	Vibration frequency f (Hz)	Vibration amplitude A (mm)	Static bed height H_0/W	Vibration strength Λ (-)
1	17.1	4.1	1.5	4.8
2	17.1	4.7	1.5	5.5
3	17.1	5.2	1.5	6.1
4	13.9	4.2	1.5	3.3
5	15.6	4.1	1.5	4
6	17.1	4	1	4.7
7	17.1	4	1.25	4.7